THE JOURNAL OF PHYSICAL CHEMISTRY C

Article

Cite This: J. Phys. Chem. C 2019, 123, 3711−3718

pubs.acs.org/JPCC

Scanning Tunneling Microscopy of the Ordered Water Monolayer on MgO(001)/Ag(001) Ultrathin Films

Michael Hollerer,[†] David Prochinig,[†] Peter Puschnig,[†] Esther Carrasco,[‡] Hans-Joachim Freund,[§] and Martin Sterrer*,[†]

[†]Institute of Physics, NAWI Graz, University of Graz, Universitätsplatz 5, 8010 Graz, Austria

[‡]IMDEA Nanoscience, Ciudad Universitaria de Cantoblanco, 28049 Madrid, Spain

[§]Department of Chemical Physics, Fritz Haber Institut der Max-Planck-Gesellschaft, Faradayweg 4-6, 14195 Berlin, Germany

ABSTRACT: Two-dimensionally ordered monolayers of water on MgO(001) have been extensively studied in the past using diffraction and spectroscopic and computational methods, but direct microscopic imaging has not been reported so far. Here, we present a scanning tunneling microscopy (STM) study, supported by infrared and X-ray photoelectron spectroscopy, of the c(4 × 2)-10H_2O and p(3 × 2)-6H_2O structures prepared on ultrathin MgO(001)/Ag(001) films. For the applied tunneling conditions, the contrast in the STM images originates from the hydroxyl groups, which result from water dissociation within the monolayer. The observed periodicities match the structures for the energetically most favorable c(4 × 2) and p(3 × 2) monolayer phases obtained from density functional calculations. Although the molecular water species within the monolayers, which are essential for the stabilization of the hydroxyl groups, could not be resolved, the STM results presented in this study provide further confirmation of the predicted structural models of the c(4 × 2)-10H_2O and p(3 × 2)-6H_2O monolayers.

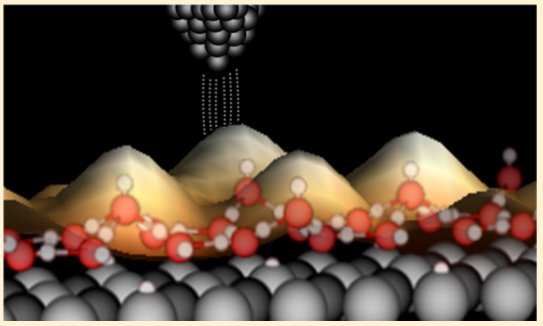

1. INTRODUCTION

The understanding of water interaction with oxide surfaces has strongly progressed over the last years. This is partly driven by the importance of water−oxide systems in a number of technological processes and also because of the fundamental interest in the general principles that govern the adsorption mode and structures of water at interfaces.[1] For water on oxides both, the nature of adsorption (molecular or dissociative) and the possibility to arrange, via hydrogen bond interaction, in two-dimensionally ordered superstructures, depend on the chemical properties of the oxides (acid−base properties), the lattice parameter, and the surface orientation and termination.[2−4] Because of the inherent complexity of the systems, it is generally not straightforward to predict how water structures evolve on a given oxide surface. Nevertheless, with the help of computational modeling and sophisticated surface science experimental investigations, detailed insight into the properties of water at selected oxide surfaces could be gained. These studies revealed, for example, the adsorption and dissociation of single water molecules,[5,6] dimerization and the formation of water clusters and agglomerates,[7,8] and the structures of 1- and 2-dimensional (2D) superstructures.[9−12]

Water adsorption on the oxides of the alkaline earth metals (MgO, CaO, and SrO) represents a particularly interesting case. They have the same crystal structure and differ only in terms of lattice constant and basicity. Hence, the influence of these parameters on the dissociation probability of water and the ability to form long-range ordered superstructures can be studied systematically. It is well established that a single water molecule adsorbs intact on the MgO(001) surface, whereas dissociation occurs on both CaO(001) and SrO(001) because of their higher basicity. An interesting trend is seen when the water coverage is increased. Computational studies have shown that 2D ordered superstructures are most stable on MgO(001), while 1-dimensional chain structures prevail on CaO(001), and isolated and dissociated monomer and dimer species represent the energetically most stable state of water on SrO(001).[13] This trend can be well explained by the differences in the interaction strength between water and the oxides and the ability to establish intermolecular hydrogen bonding. Recent scanning tunneling microscopy (STM) studies have confirmed the presence of 1-dimensional chain structures of water on CaO(001)[13] and of monomer and dimer species on an SrO(001)-terminated $Sr_3Ru_2O_7$ surface[6] at room temperature. Direct microscopic observation of the 2D water structures on MgO(001) is, however, still missing. Herein, we report on a first attempt to resolve the 2D ordered monolayer structures formed on MgO(001) by STM.

In Figure 1, we present models of the two most stable water monolayer structures on MgO(001), the high-coverage c(4 × 2)-10H_2O and the low-coverage p(3 × 2)-6 H_2O. Early

Received: December 20, 2018
Revised: January 17, 2019
Published: January 17, 2019

DOI: 10.1021/acs.jpcc.8b12256
J. Phys. Chem. C 2019, 123, 3711−3718

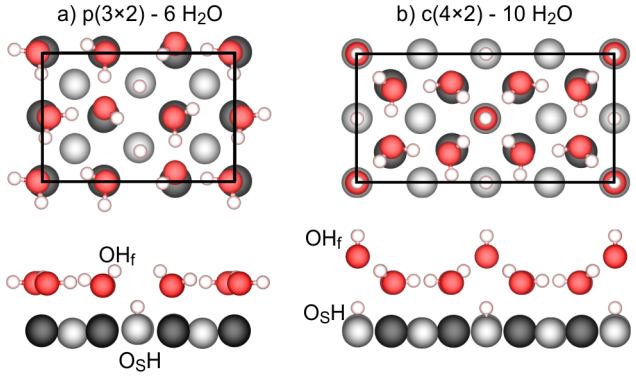

Figure 1. Top and side views of the most stable (3 × 2) and (4 × 2) water structure models on MgO(001). (a) p(3 × 2)-6H_2O; (b) c(4 × 2)-10H_2O. (Mg dark gray; O light gray and red; and H white).

experiments with MgO(001) single crystal surfaces using diffraction methods[12,14] have revealed the symmetries and sizes of the unit cells of these structures, and thermal desorption experiments[15] have shown that the water monolayer is stable up to 210 K in ultrahigh vacuum (UHV). The phase transition between the c(4 × 2) and the less-dense p(3 × 2) phase occurs at around 180 K. The molecular-level details of the arrangement of individual water/hydroxyl species within these structures could, however, only be obtained with the help of calculations using density functional theory (DFT). While the early structural proposal for the p(3 × 2)-6H_2O by Giordano et al.[16] (Figure 1a) is still accepted, many different models of the c(4 × 2) structure have been suggested over the years, but a conclusive structural model (Figure 1b) has only been obtained after extensive structural search using DFT in combination with infrared spectroscopic experiments.[17] A common feature of the monolayer structures is that they contain both molecularly and dissociatively adsorbed water, that is, they are mixed water/hydroxyl phases. The dissociation products give rise to two inequivalent hydroxyl groups, the "surface OH" (O_SH) resulting from the binding of the proton to a lattice oxygen and the "free OH" (OH_f). As shown in Figure 1, the OH_f groups are stabilized by hydrogen-bond interaction with the surrounding H_2O molecules. For the c(4 × 2)-10H_2O in particular, the stabilized OH_f groups strongly protrude out of the monolayer plane consisting of nearly horizontally aligned H_2O molecules.[17]

Because of the insulating nature of bulk MgO, STM investigations are limited to ultrathin MgO(001) films grown on a metallic substrate, for example, Ag(001) or Mo(001). The properties and reaction paths of adsorbates on oxide surfaces may, however, be significantly different when the oxide is prepared in the form of a metal-supported ultrathin film compared to bulk.[18] In particular, MgO(001) ultrathin films have evolved to the prototypical system for studying charge-transfer processes between the metal substrate and adsorbates through a wide band gap dielectric interlayer.[19] Various adsorbates with moderate to high electron affinity, including Au,[20,21] O_2,[22] NO_2[23] and pentacene,[24] have been shown to be negatively charged on metal-supported MgO(001) ultrathin films. Several experimental studies have also treated water adsorption on ultrathin MgO(001)/Ag(001) films from the single-molecule level to hydroxylation at elevated water vapor pressure,[25−28] and it was generally concluded that water dissociation is enhanced on ultrathin MgO films compared to bulklike MgO(001). Shin et al. and Cabailh et al. studied water adsorption and dissociation on monolayer and submonolayer MgO(001)/Ag(001) films with STM.[25,28] It was found that intact water molecules adsorb at low temperature (10 K) without any tendency to form ordered structures on regular MgO(001) terraces. STM tip-induced dissociation results in adsorbed hydroxyl species, which appear in STM images with much less contrast than molecular water.[28,29] On the other hand, water dissociation occurs spontaneously at the borders of submonolayer MgO islands, resulting in their decoration with hydroxyl groups that are easily observed in STM.[25] According to DFT calculations, the water monomer adsorption on ultrathin MgO(001) films is not particularly affected by the presence of the Ag(001) support, and dissociation of the water monomer, although energetically more preferred than on bulk MgO(001), is still slightly endothermic.[30] The situation changes when water dimers are considered. On 1 ML MgO(001)/Ag(001), the dissociation of one water molecule in the dimer is energetically favorable, and the dissociated state is stabilized compared to bulk MgO(001) because of the polaronic distortion of the thin film induced by the charged fragments.[31] In addition, the calculated adsorption energy of the dissociated dimer is only slightly smaller than that of a full p(3 × 2) monolayer [E_{ads} = 0.75 eV for the dissociated dimer on 1 ML MgO(001)/Ag(001)[31] versus E_{ads} = 0.81 eV for the p(3 × 2)-6H_2O on 2 ML MgO(001)/Ag(001)[30]], and hence, the propensity to form long-range ordered water structures might be affected on ultrathin MgO(001) films.

In this work, we study water adsorption on ultrathin MgO(001) films supported on Ag(001) with emphasis on the formation and structure of long-range ordered water monolayer phases, using infrared reflection absorption spectroscopy (IRAS), X-ray photoelectron spectroscopy (XPS), and low-temperature STM. Our IRAS and XPS results confirm that water monolayer phases exhibit the same properties on ultrathin (2 ML) and more bulklike (12 ML) MgO films, and with STM, we are able to image both known stable water monolayer phases on MgO(001). STM image simulations using the Tersoff−Hamann approach support our experimental observations.

2. EXPERIMENTAL AND COMPUTATIONAL DETAILS

Experiments were conducted in two separate UHV setups. The first setup was mainly used for spectroscopic studies and has, in addition to the standard components for sample preparation and characterization, a Bruker IFS66v infrared spectrometer for IRAS studies and a dual-anode (Mg/Al) X-ray source together with a hemispherical electron analyzer (SPECS PHOIBOS 150) for X-ray photoelectron spectroscopy (XPS) experiments attached. Low-temperature STM experiments were performed in a separate UHV setup consisting of a preparation chamber and a CreaTec low-temperature scanning tunneling microscope operated at liquid N_2 or liquid He temperature. Magnesium oxide (MgO) was epitaxially grown in varying thicknesses on a supporting Ag(001) crystal. Ag(001) was cleaned by repeated cycles of Ar^+ sputtering (800 V, ∼5 μA) and annealing (773 K) until defined (1 × 1) spots were observed in low-energy electron diffraction (LEED). MgO(001) thin films were grown by evaporation of Mg (rate 0.67 ML/min) on Ag(001) at 573 K in an oxygen background of 1 × 10^{-6} mbar. To obtain wide terraces, the sample was slowly cooled to room temperature after film growth.[32] The slow cooling procedure was not applied for the samples used for spectroscopy experiments and, thus, they

DOI: 10.1021/acs.jpcc.8b12256
J. Phys. Chem. C 2019, 123, 3711−3718

exhibit a higher degree of defectiveness than the samples used for STM experiments. Order and cleanliness of the MgO(001)/Ag(001) thin film was checked with LEED and XPS. Water (H_2O and D_2O) was dosed via a precision valve from a glass vial attached to the UHV chamber and properly degassed before dosing by repeated freeze−pump−thaw cycles. For spectroscopic measurements, a multilayer of water was first adsorbed via background-dosing of D_2O at a substrate temperature of 100 K. IR spectra were then collected for the stated annealing temperatures with a resolution of 4 cm^{-1} by accumulation of 1000 scans. A spectrum of the clean surface was used for background correction. XPS data were obtained with an Al Kα X-ray source ($h\nu$ = 1486.6 eV, 100 W) at a photoelectron takeoff angle of 60°. X-ray irradiation induces a local heating effect, which can be estimated to be about 5 K based on infrared spectroscopy, but did not lead to additional water dissociation within the monolayer structures.[17] To obtain a defined water monolayer for STM measurements, the substrate was kept at 155−160 K during water dosing. After water adsorption, the sample was quickly transferred to the STM system, where it was cooled to 77 or 5 K.

Density functional calculations were performed for the p(3 × 2)-6H_2O and c(4 × 2)-10H_2O structural models shown in Figure 1a,b, respectively. Starting from the adsorption geometry reported in ref 17 and using the repeated slab approach, we have computed the relaxed geometry for the p(3 × 2)-6H_2O and c(4 × 2)-10H_2O structures on 2 ML of MgO(001) on Ag(001), where the latter has been modeled by five atomic Ag layers. Utilizing the VASP code,[33,34] the generalized gradient approximation (GGA)[35] is used for exchange−correlation effects, and van der Waals corrections according to the DFT-D3 method of Grimme have been added.[36] Using the projector-augmented wave method, a plane-wave cutoff of 400 eV is employed, and for k-point sampling, a Monkhorst−Pack grid of 6 × 9 × 1 points is used with a first-order Methfessel−Paxton smearing of 0.1 eV for Brillouin zone integrations. The STM simulations are performed within the framework of the Tersoff−Hamann approximation[37] by computing the local density of states in an energy window from the Fermi energy to either 2 eV above or 2 eV below, respectively. Noncontact atomic force microscopy (nc-AFM) images have been simulated by applying the probe-particle model[38] and using a CO molecule as the probe particle with an effective charge of −0.05.

3. RESULTS AND DISCUSSION

3.1. Spectroscopic Characterization of Ordered Water Phases on 2 ML MgO(001)/Ag(001). Spectroscopically, the two ordered monolayer phases of water on MgO(001) can be distinguished based on the different stretching frequencies of the hydroxyl and water species. As reference, we present in Figure 2 (bottom) the experimental IRA spectrum for the water monolayer prepared on a 12 ML thick, bulklike MgO(001)/Ag(001) film at 163 K. (Note that the experiments were performed with D_2O instead of H_2O.) The spectrum shows narrow bands in the range 2600−2750 cm^{-1} and broad absorptions between 2000 and 2500 cm^{-1}. The individual spectral contributions can be assigned based on the good agreement between the experimentally observed IR bands and the calculated OD stretching frequencies of the most stable structures shown in Figure 1a,b.[17] While the OD_f groups in both structures have similar stretching frequencies at 2720 cm^{-1}, the O_SD groups are slightly different, 2638 cm^{-1} for c(4 × 2)-10H_2O and 2595 cm^{-1} for p(3 × 2)-6H_2O. Because of the metal surface selection rule, the molecular water species, which are oriented almost parallel to the surface in both structures, give rise to only weak absorption signals. In fact, they do not contribute to the IR spectrum of the p(3 × 2) structure. In the case of the c(4 × 2) structure, combinations of the symmetric and antisymmetric D_2O stretching vibrations lead to signal contributions in the 2100−2450 cm^{-1} spectral range, which are detected in the experiment as broad bands. The additional absorption at around 2532 cm^{-1} in the spectrum of D_2O on 12 ML MgO(001)/Ag(001) is not related to the ordered monolayer phases. Its origin will be discussed in the next paragraph when the IRAS results for D_2O on an ultrathin MgO(001)/Ag(001) film are presented.

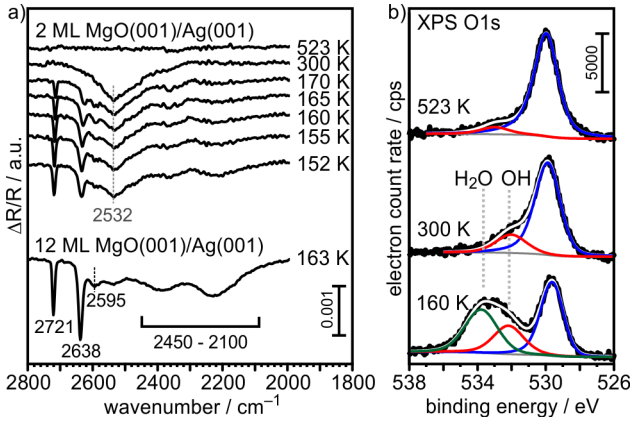

Figure 2. (a) IRA spectra of the water (D_2O) monolayer on 12 ML MgO(001)/Ag(001) (bottom) and 2 ML MgO(001)/Ag(001) (top). D_2O was dosed at 100 K, and spectra were recorded after heating to the temperature indicated in the figure. (b) XP spectra (O 1s region) of 2 ML MgO(001)/Ag(001) after initial adsorption of D_2O at 100 K and subsequent heating to the indicated temperature.

A series of IRA and XP spectra of 2 ML MgO(001)/Ag(001) recorded after initial adsorption of water (D_2O) multilayers at 100 K and subsequent heating to the indicated temperatures in vacuum is shown in Figure 2a(top) and 2b. Because multilayer desorption occurs at 150 K, the observed spectral features can be attributed to the monolayer water species. The XP spectrum presented in Figure 2b reveals, in addition to the oxide O 1s peak at 529.6 eV binding energy (BE), the presence of a hydroxyl species with 532.4 eV BE and molecular water with 533.9 eV BE, confirming the mixed molecular/dissociated nature of the monolayer phase. The smaller intensities of the OD and D_2O vibrations in the IRA spectrum of the ultrathin film compared to the 12 ML thick film observed experimentally is in agreement with the prediction from DFT.[30] The positions of the O_SD and OD_f signals are the same on both substrates, as shown earlier.[26]

The evolution of the water monolayer-related vibrations with increasing temperature (Figure 2a, 152−170 K) observed in the present study for the ultrathin MgO film follows the same trend as previously reported for a 12 ML thick MgO(001)/Ag(001) film, suggesting the predominance of the c(4 × 2) phase at lower temperature and a partial transition c(4 × 2) → p(3 × 2) at increasing temperature.[17] Because of the smaller intensities of the water monolayer-related vibrations, the previously mentioned broad band at 2532 cm^{-1} appears more prominent in the spectra of the 2 ML MgO(001)/Ag(001) sample. This band remains present upon

DOI: 10.1021/acs.jpcc.8b12256
J. Phys. Chem. C 2019, 123, 3711−3718

heating to 300 K but disappears after annealing at 523 K. The corresponding XP spectrum of the film heated to 300 K shows noticeable intensity of the hydroxyl O 1s species (about 20% of the full monolayer, Figure 2b). In agreement with previous studies, we attribute these hydroxyl species to water adsorption and dissociation at the nonpolar [100] step sites of MgO.[25,39] Steps are indeed the most abundant defects on the thin film sample and exhibit higher reactivity toward water dissociation than the (100) terrace sites.[40] The disappearance of the IRAS signal at 2532 cm^{-1} and the hydroxyl O 1s XPS signal after heating to 523 K well agrees with the reported stability of hydroxyl species at steps obtained from DFT calculations.[39]

3.2. STM of the Ordered Water Phases on 2 ML MgO(001)/Ag(001). The spectroscopic results presented above confirm that the water monolayer phases exhibit the same properties and structures on an ultrathin MgO(001) film and on bulklike MgO(001). For the STM investigations presented in the following, we have therefore grown MgO(001) films with a nominal thickness (2 ML) similar to that used in the spectroscopic investigations. An STM image of the clean surface of a MgO(001)/Ag(001) film is shown in Figure 3a. It exhibits flat terraces of up to 70 nm width,

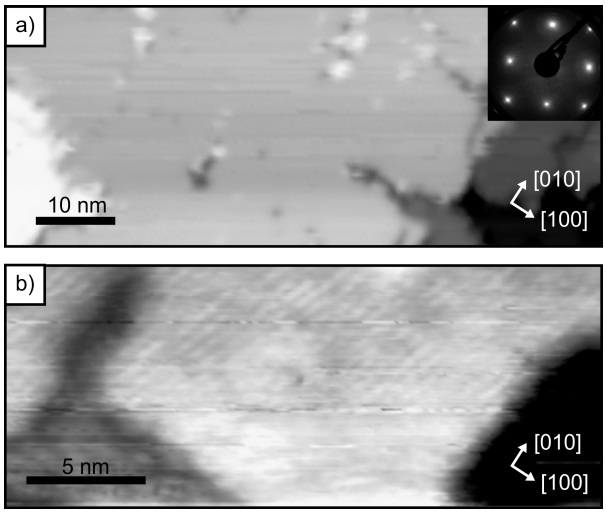

Figure 3. STM images taken at 5 K of 2 ML MgO(001)/Ag(001) before (a) and after (b) adsorption of D_2O at 160 K. (a) 75 nm × 30 nm, V_s = +3.0 V, i_t = 100 pA, (b) 25 nm × 10 nm, V_s = −0.72 V, i_t = 30 pA. [The inset in (a) shows the LEED pattern of the MgO(001)/Ag(001) film taken at E = 90 eV].

sufficiently large to enable the formation of long-range ordered superstructures. For preparation of the water monolayer, we used a slightly different water dosing procedure compared to the spectroscopy measurements. Instead of water multilayer adsorption at 100 K and subsequent heating, we saturated the MgO surface with water directly at a sample temperature of 155−160 K, which is slightly above the multilayer desorption temperature but well below monolayer desorption, and then quickly cooled the sample to liquid helium temperature inside the STM compartment. By using this procedure and according to the infrared results presented in Figure 2a, we expect to predominantly form the c(4 × 2) phase under these conditions.

A larger scale STM image of such a preparation is shown in Figure 3b, which presents a water-covered MgO(001) terrace separated from neighboring terraces by monolayer (on the left-hand side) and bilayer (on the right-hand side) steps. Because the step edges of the MgO islands run along the non-polar ⟨100⟩ directions, the high-symmetry axes of the substrate can be straightforwardly identified. We note that the island terrace is not flat but exhibits a distinct periodic corrugation that points to the presence of a superstructure formed by the adsorbed water. In Figure 4a, where a detail of the MgO(001)

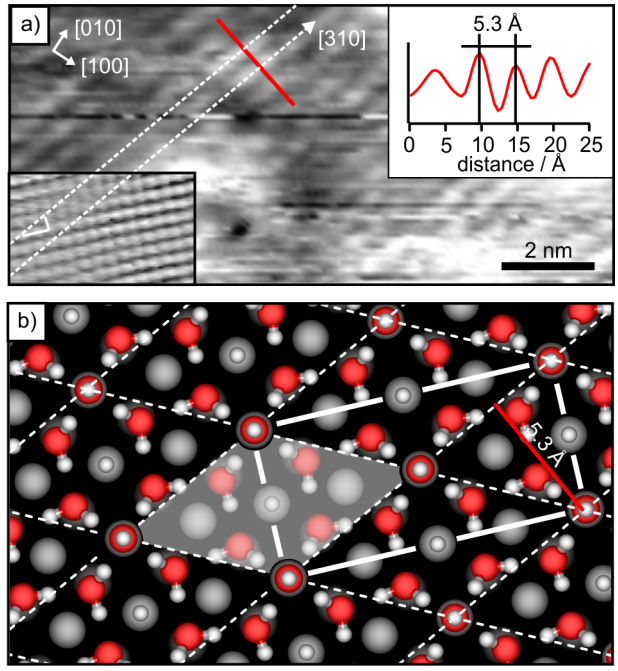

Figure 4. (a) Detail (13 nm × 6 nm) of the STM image shown in Figure 3b. The inset is an atomically resolved image (4 nm × 2.4 nm) of the MgO(001) surface obtained from the same sample. The scale bar applies to both STM images displayed in (a). The stripes in the STM image run along the [310] substrate direction (dashed white lines). Neighboring stripes exhibit a perpendicular separation of 5.3 Å (see line scan). (b) Model of the c(4 × 2)-10H_2O structure with the conventional rectangular c(4 × 2) unit cell and corresponding primitive rhombic unit cell. (Mg dark gray; O light gray and red; and H white).

terrace is shown with enhanced contrast, the superstructure is identified as parallel stripes with a perpendicular separation of about 5.3 Å (see line profile in Figure 4a). In addition, the stripes appear to be not aligned along a high-symmetry axis of the substrate.

To confirm the substrate orientation and determine the stripe direction exactly, we have obtained from the same preparation an atomically resolved image of the MgO(001) substrate (see inset in Figure 4a). Typically, only one ionic sublattice is resolved, most likely representing the positions of the oxygen ions.[41] From Figure 4a, we have extracted the stripe orientation and overlaid it onto the ionic lattice. The stripes are rotated from the [110] direction by 26.5°. Close inspection of Figure 4a reveals that neighboring stripes are separated by two lattice constants in the [110] direction and one lattice constant in the $[\bar{1}10]$ direction. Thus, the stripes form a commensurate superstructure with respect to the underlying MgO lattice. The stripe direction can be identified as the [310] substrate direction (Figure 4a).

Coming back to the models of the ordered water overlayers shown in Figure 1, we note that the [310] direction is the

DOI: 10.1021/acs.jpcc.8b12256
J. Phys. Chem. C 2019, 123, 3711−3718

diagonal of the conventional c(4 × 2) unit cell and represents the direction of the principle lattice vector of the corresponding primitive rhombic unit cell, which in matrix notation reads $\begin{pmatrix} 2 & -1 \\ 2 & 1 \end{pmatrix}$. To better illustrate this, we present in Figure 4b a model of the c(4 × 2)-10H_2O phase with the conventional unit cell marked by the rectangle and the corresponding primitive unit cell represented by the gray area. The unit cell vectors of the primitive unit cell have a length of 6.66 Å (assuming a bulk lattice constant of MgO, a = 2.98 Å) and each encloses an angle of 26.57° with the [110] substrate direction. Note that the perpendicular distance between the parallel sides of the rhombus is 5.3 Å, similar to the experimentally observed stripe separation in Figure 4a. Combining all this information provides strong support for the conclusion that the stripe superstructure imaged in Figure 3b represents the ordered c(4 × 2) water monolayer phase on MgO(001).

Attempts to better resolve the c(4 × 2) phase with STM were often not successful because of the presence of mobile adsorbates on the surface, which led to unstable tip conditions and streaky or blurred image appearance. An STM image of a water-covered MgO(001) terrace with the stripe superstructure, which exhibits some areas where better resolution has been obtained, is shown in Figure 5a. The [310] stripe

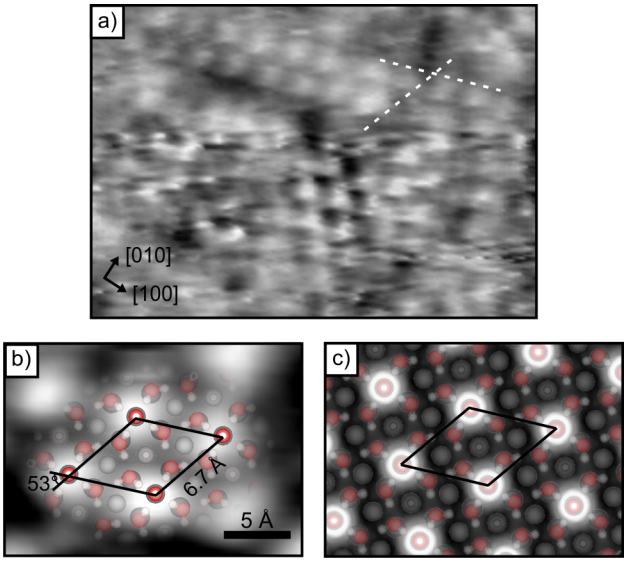

Figure 5. (a) STM image taken at 5 K (8.1 nm × 5.7 nm, V_s = −1.1 V, i_t = 50 pA) of the water monolayer on 2 ML MgO(001)/Ag(001). The dashed lines represent the [310] substrate directions. (b) Detail (2.2 nm × 1.6 nm) of (a) with an overlaid model of the c(4 × 2)-10H_2O structure. (c) Simulated STM image (V_{bias} = −1 V) of the c(4 × 2)-10H_2O structure.

directions are indicated by dashed lines. The individual protrusions are arranged in a rhombic lattice spanned by the ⟨310⟩ family of substrate directions. A detail of Figure 5a showing four protrusions arranged in the rhombic form is presented in Figure 5b. The side length and enclosed angles of the rhombus perfectly fit the dimension and angles of the primitive unit cell of the c(4 × 2) structure. What remains to be determined is the identity of the protrusions. We note that the primitive unit cell contains five water molecules, out of which four are molecular water and one is dissociated. Because we image only one protrusion per primitive unit cell, we exclude molecular water and assign the protrusions to the OH_f groups of the c(4 × 2)-10H_2O structure as they are the most obvious protruding element of this structure from a geometrical point of view (Figure 1b). To support this assignment, we compare our experimental STM images with simulated images of the c(4 × 2)-10 H_2O structure, which have been obtained by applying the Tersoff–Hamann approximation (Figure 5c). Because of the absence of molecular states for water and hydroxyl groups at bias voltages around the Fermi level, the contrast in the simulated image is entirely geometric in nature and determined by the protruding OH_f groups, thus confirming our assignment.

In addition to regions on the surface of the MgO(001)/Ag(001) thin film, where the long-range ordered c(4 × 2)-10H_2O phase grows on larger MgO(001) terraces in a single rotational domain (see Figure 3b), we also found areas, such as the one shown in the STM image of Figure 6a, that appear to

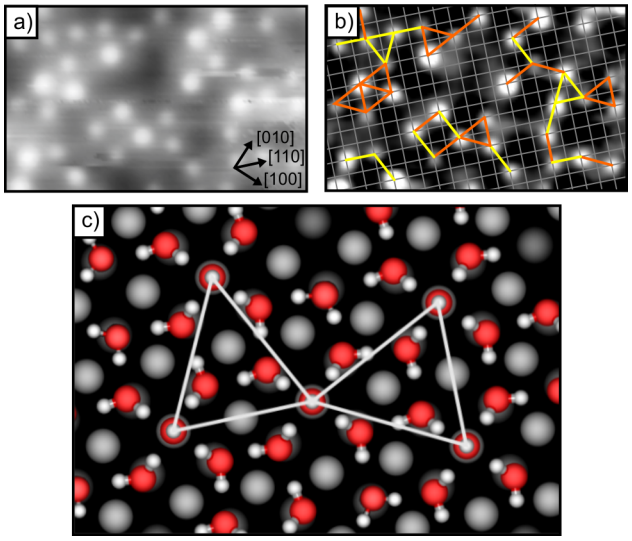

Figure 6. (a) STM image taken at 77 K (6.1 nm × 3.7 nm, V_s = −0.26 V, i_t = 50 pA) of water on 2 ML MgO(001)/Ag(001). (b) Same area as in (a) displayed with enhanced contrast and with an overlaid ionic sublattice of MgO(001). All protrusions are located at the same kind of lattice site. The lines connect nearest neighbor protrusions and the different colors represent the two different rotational domain alignments. (c) Model for the cluster formed by two corner-sharing triangular structures [middle-right in (b)] constructed with the basic structural unit of the c(4 × 2)-10H_2O structure. (Mg dark gray; O light gray and red; and H white).

exhibit, as judged by the number of protrusions observed, less water coverage and less order. Indeed, the appearance of Figure 6a strongly resembles that of STM images for individual water molecules on MgO thin films reported earlier by Shin et al.[28] However, a closer inspection of this image reveals that the protrusions are not randomly spread over the surface area but arranged in groups that exhibit the general structural motif of the c(4 × 2)-10H_2O phase. To illustrate this point, we have overlaid an ionic sublattice of the MgO(001) surface onto the STM image and centered one lattice point on one of the protrusions. As shown in Figure 6b, all observed protrusions are aligned with the ionic sublattice. In addition, nearest neighbor distances and position vectors appear mainly in two groups, the next nearest neighbors in the ⟨110⟩ directions and the nearest neighbors in the ⟨310⟩ directions, thus representing the lattice directions and points of the c(4 × 2) structure in the

DOI: 10.1021/acs.jpcc.8b12256
J. Phys. Chem. C 2019, 123, 3711−3718

two possible rotational domains. We, therefore, assign the protrusions to the protruding OH_f groups of the c(4 × 2)-10H_2O structure.

In Figure 6b, we have connected neighboring protrusions with differently colored lines according to their domain alignment. From this representation it becomes clear that in this particular image area the water molecules and hydroxyl groups are arranged in clusters where the short-range order is maintained. Within the clusters, small units of the c(4 × 2) structure, most often not extending to a complete c(4 × 2) unit cell size, are directly linked with small units aligned along the other, 90°-rotated domain.

At this point, it is interesting to think about how the water molecules in the overlayer have to rearrange, or if they have to rearrange at all, to form the observed clusters. From previous DFT calculations, which have dealt with the water coverage-dependent formation of ordered (3 × 2) and (4 × 2) phases on the MgO(001) surface, it is known that protruding OH_f groups also exist in structures with slightly lower coverage than c(4 × 2)-10H_2O, namely, p(4 × 2)-9H_2O and p(3 × 2)-7H_2O.[17] These structures are, however, energetically slightly less favorable than the c(4 × 2)-10H_2O phase. Nevertheless, these results show that the factors that govern the formation and stability of the protruding OH_f are, apart from the molecule−adsorbate interaction, the hydrogen-bond interaction of OH_f with the hydrogen atoms of the four water molecules in the first coordination sphere (see Figure 1b). Hence, it is tempting to construct a molecular model for the structures observed in Figure 6a using this principal structural unit of the c(4 × 2)-10H_2O. As an example, we show in Figure 6c our model for the two corner-sharing triangular structures, where each triangle represents half of the primitive c(4 × 2) unit cell in the respective domain. Only one water molecule in the first coordination sphere of the central OH_f group has to be rotated to establish a continuous hydrogen bonding network over the two 90° rotated domains. While other arrangements of water molecules around the OH_f groups are probably conceivable, this simple analysis demonstrates that, if at all, only very minor geometrical rearrangements compared to the original c(4 × 2) structural motif are necessary to be able to construct molecular models of the short-range ordered water/hydroxyl clusters present on the surface. The energetic cost for the necessary rearrangements are expected to be minute, which explains why the structures are stable and do not relax into the energetically more unfavorable lower coverage structures at the temperature of the experiment.

According to the IRAS data presented in Figure 2a and considering the experimental conditions for water monolayer preparation (160 K adsorption temperature), we may, however, also find the lower coverage p(3 × 2)-6H_2O phase. In comparison with the c(4 × 2)-10H_2O, the p(3 × 2)-6H_2O structure is much less corrugated and the two OH_f groups in the unit cell protrude only slightly out of the otherwise flat water layer (Figure 1a). Identification of the p(3 × 2)-6H_2O structure by STM is hence likely to be more difficult. In Figure 7a, we show a detail of an STM image, where protrusions do not form a rhombic lattice but instead are arranged in zig-zag lines along the ⟨110⟩ direction with neighboring protrusions connected along ⟨100⟩.

Overlaying a grid representing an ionic sublattice of the MgO(001) surface reveals that the protrusions are indeed separated by only nearest neighbor distances in ⟨100⟩ directions (Figure 7b), which corresponds to the arrangement

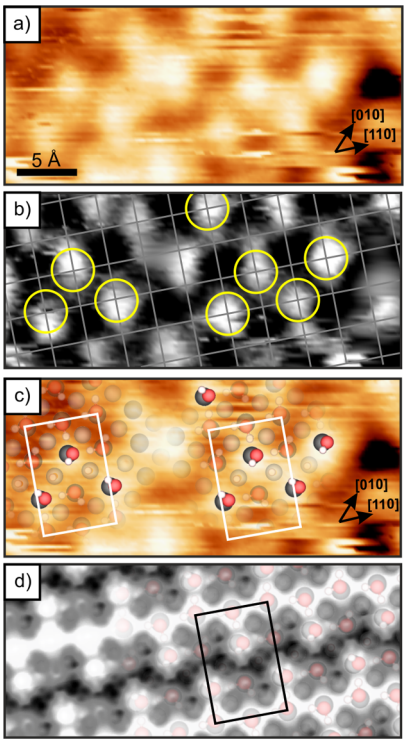

Figure 7. (a) STM image taken at 77 K (3.3 nm × 1.5 nm, V_s = −0.53 V, i_t = 50 pA) of water on 2 ML MgO(001)/Ag(001). As shown in (b), the protrusions are arranged in zig-zag lines with a nearest neighbor separation of one lattice constant in [100] directions. [The grid represents a sublattice of the MgO(001) substrate.] (c) Same STM image as in (a) with an overlaid model of the p(3 × 2)-6H_2O structure. The protrusions observed in the STM image fit to the expected lattice position of the OH_f groups. (d) Simulated STM image (V_{bias} = −1 V) of the p(3 × 2)-6H_2O structure.

of the OH_f groups in the p(3 × 2)-6H_2O unit cell. We note that a theoretically proposed p(3 × 2) structure with eight water molecules per unit cell, with two dissociated molecules and OH_f groups protruding out of the water layer similar as in the c(4 × 2)-10H_2O structure, would give rise to a similar zig-zag appearance.[17] However, this structure is energetically very unfavorable. In addition, we find the apparent height of the protrusions shown in the STM image in Figure 7a to be smaller than those of the c(4 × 2)-10H_2O structure. Therefore, we attribute the features in Figure 7a to small water clusters that contain the basic structural motif of p(3 × 2)-6H_2O (Figure 7c). Again, our interpretation is supported by comparison of the experimental image with the simulated STM image in Figure 7d, where it is shown that the slightly upward tilted OH_f groups give rise to a zig-zag-like contrast. However, in addition to the OH_f groups, the neighboring molecular water species, which form stripes along the [110] directions, show up with considerable intensity in the simulation for negative bias voltage corresponding to filled-state imaging (Figure 7d). This might, however, be due to a slight overestimation of the contribution of the highest occupied molecular orbital of molecular water in the GGA calculations. Generally, we expect the image contrast around the Fermi level to be mainly determined by geometrical factors because of the absence of molecular states.

Our STM results on the structure of the water monolayer on MgO(001) are in agreement with the models of the c(4 × 2)-10H_2O and p(3 × 2)-6H_2O structures previously proposed

DOI: 10.1021/acs.jpcc.8b12256
J. Phys. Chem. C 2019, 123, 3711−3718

from DFT calculations. For the applied tunneling conditions, the STM image contrast is determined by the protruding OH_f groups, and the observed periodicities are in agreement with those expected for the arrangement of the OH_f groups in the c(4 × 2)-10H_2O and p(3 × 2)-6H_2O structures. Further confirmation of the structural models would require a simultaneous, or at least consecutive, imaging of OH_f's and the surrounding molecular water. STM image simulations reveal that the vertically aligned OH_f's determine the image contrast of the c(4 × 2)-10H_2O structure in a wide range of bias voltages because of geometrical reasons (Figure 8a). In

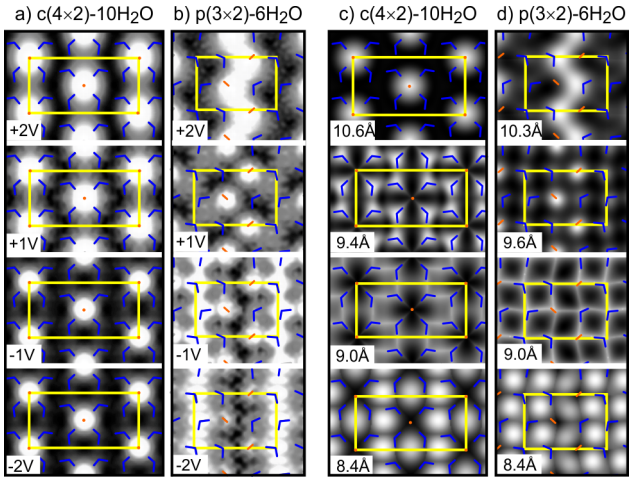

Figure 8. Simulated STM (a,b) and nc-AFM images (c,d) of the c(4 × 2)-10H_2O and p(3 × 2)-6H_2O structures. The images have been generated for the bias voltages (STM) and tip-sample distances Δz (nc-AFM) indicated in the figure. Δz is the distance between the surface MgO plane and the oxygen atom of the CO-tip. Yellow rectangles represent the unit cells of the structures and the positions of the water molecules (blue) and OH_f groups (orange) are indicated.

contrast, in the p(3 × 2) structure, the distinct OH_f contrast is only obtained for empty state images, whereas in filled state images also molecular water is visible (Figure 8b). However, such contrast has not been observed experimentally and, as mentioned above, could be due to an artifact of the calculation.

Ultimately, nc-AFM with CO-functionalized tips could provide the required information on molecular water species within the 2D phases. nc-AFM has recently been applied to the investigation of water clusters on, for example, thin NaCl(100) films and Fe_3O_4(001) surfaces.[8,42] As an outlook for future nc-AFM studies of the water monolayers on MgO(001), we present in Figure 8c,d simulated nc-AFM images of the c(4 × 2)-10H_2O and p(3 × 2)-6H_2O structures, obtained by applying the probe-particle model.[38] For c(4 × 2)-10H_2O (Figure 8c), the simulations reveal that at a large tip-sample distance (Δz), the image contrast is determined by the OH_f groups, similar as in our STM studies. At slightly closer distance, a contrast reversal occurs, and triangular features representing the water molecules appear, which may even allow the orientation of the water molecules to be determined. Interestingly, the model predicts a different Δz dependence for the p(3 × 2) structure (Figure 8d). Here, OH_f's dominate at intermediate Δz, giving rise to a zig-zag appearance similar as in our STM images (Figure 7), whereas at larger distances also a zig-zag line appears, which, however, originates from the molecular water species. At a closer approach, the model predicts for both structures the observation of sharp lines and, finally, again a contrast inversion, which can be explained by Pauli repulsion and lateral relaxation of the probe particle.

4. CONCLUSIONS

In conclusion, our low-temperature STM study of water monolayers on ultrathin MgO(001)/Ag(001) films revealed morphological signatures that are in agreement with the models of the c(4 × 2)-10H_2O and p(3 × 2)-6H_2O structures predicted for bulk MgO(001). Furthermore, IRAS confirmed the similarity of the water monolayers on ultrathin and bulklike MgO(001) films. Thus, we conclude that the structural properties of the water monolayers are not affected by the MgO film thickness and possible charge transfer through the film.

Our STM images show that the c(4 × 2)-10H_2O monolayer grows in single-domain orientation on large MgO(001) terraces. However, also metastable water/hydroxyl clusters have been found, which often consist of directly linked, 90°-rotated c(4 × 2) units. The present study provides further proof of the predicted structures of water monolayers on MgO(001), in particular regarding the position and arrangement of the OH_f groups within the unit cells. Because nc-AFM image simulations reveal distinct H_2O and OH^- contrast for different tip-sample distances, we suggest that additional information about the orientation of the molecular water within the monolayer could be obtained in the future by using nc-AFM with CO-functionalized tips.

AUTHOR INFORMATION

Corresponding Author

*E-mail: martin.sterrer@uni-graz.at.

ORCID

Peter Puschnig: 0000-0002-8057-7795

Hans-Joachim Freund: 0000-0001-5188-852X

Martin Sterrer: 0000-0001-9089-9061

Notes

The authors declare no competing financial interest.

ACKNOWLEDGMENTS

Financial support from the Austrian Science Fund (FWF) project I3731 is acknowledged. The computational results presented have been achieved using the computing facilities of the University of Graz and the Vienna Scientific Cluster (VSC3).

REFERENCES

(1) Björneholm, E.; Hansen, M. H.; Hodgson, A.; Liu, L. M.; Limmer, D. T.; Michaelides, A.; Pedevilla, P.; Rossmeisl, J.; Shen, H.; Tocci, G.; et al. Water at interfaces. *Chem. Rev.* **2016**, *116*, 7698−7726.

(2) Hu, X. L.; Carrasco, J.; Klimeš, J.; Michaelides, A. Trends in water monomer adsorption and dissociation on flat insulating surfaces. *Phys. Chem. Chem. Phys.* **2011**, *13*, 12447−12453.

(3) Rao, R. R.; Kolb, M. J.; Hwang, J.; Pedersen, A. F.; Mehta, A.; You, H.; Stoerzinger, K. A.; Feng, Z.; Zhou, H.; Bluhm, H.; et al. Surface orientation dependent water dissociation on rutile ruthenium dioxide. *J. Phys. Chem. C* **2018**, *122*, 17802−17811.

(4) Schwarz, M.; Faisal, F.; Mohr, S.; Hohner, C.; Werner, K.; Xu, T.; Skála, T.; Tsud, N.; Prince, K. C.; Matolín, V.; et al. Structure-dependent dissociation of water on cobalt oxide. *J. Phys. Chem. Lett.* **2018**, *9*, 2763−2769.

DOI: 10.1021/acs.jpcc.8b12256
J. Phys. Chem. C 2019, 123, 3711−3718

(5) Brookes, I. M.; Muryn, C. A.; Thornton, G. Imaging water dissociation on TiO_2(110). *Phys. Rev. Lett.* **2001**, *87*, 266103.
(6) Halwidl, D.; Stöger, B.; Mayr-Schmölzer, W.; Pavelec, J.; Fobes, D.; Peng, J.; Mao, Z.; Parkinson, G. S.; Schmid, M.; Mittendorfer, F.; et al. Adsorption of water at the SrO surface of ruthenates. *Nat. Mater.* **2016**, *15*, 450−455.
(7) Merte, L. R.; Bechstein, R.; Peng, G.; Rieboldt, F.; Farberow, C. A.; Zeuthen, H.; Knudsen, J.; Lægsgaard, E.; Wendt, S.; Mavrikakis, M.; et al. Water clustering on nanostructured iron oxide films. *Nat. Commun.* **2014**, *5*, 4193.
(8) Meier, M.; Hulva, J.; Jakub, Z.; Pavelec, J.; Setvin, M.; Bliem, R.; Schmid, M.; Diebold, U.; Franchini, C.; Parkinson, G. S. Water agglomerates on Fe_3O_4(001). *Proc. Natl. Acad. Sci. U.S.A.* **2018**, *115*, E5642−E5650.
(9) Mu, R.; Zhao, Z.-j.; Dohnálek, Z.; Gong, J. Structural motifs of water on metal oxide surfaces. *Chem. Soc. Rev.* **2017**, *46*, 1785−1806.
(10) Mirabella, F.; Zaki, E.; Ivars-Barceló, F.; Li, X.; Paier, J.; Sauer, J.; Shaikhutdinov, S.; Freund, H.-J. Cooperative formation of long-range ordering in water ad-layers on Fe_3O_4(111). *Angew. Chem., Int. Ed.* **2018**, *57*, 1409−1413.
(11) Meyer, B.; Marx, D.; Dulub, O.; Diebold, U.; Kunat, M.; Langenberg, D.; Wöll, C. Partial dissociation of water leads to stable superstructures on the surface of zinc oxide. *Angew. Chem., Int. Ed.* **2004**, *43*, 6641−6645.
(12) Heidberg, J.; Redlich, B.; Wetter, D. Adsorption of water vapor on the MgO(100) single crystal surface. *Ber. Bunsen-Ges. Phys. Chem.* **1995**, *99*, 1333−1337.
(13) Zhao, X.; Shao, X.; Fujimori, Y.; Bhattacharya, S.; Ghiringhelli, L. M.; Freund, H.-J.; Sterrer, M.; Nilius, N.; Levchenko, S. V. Formation of water chains on CaO(001): What drives the 1D growth? *J. Phys. Chem. Lett.* **2015**, *6*, 1204−1208.
(14) Ferry, D.; Glebov, A.; Senz, V.; Suzanne, J.; Toennies, J. P.; Weiss, H. Observation of the second ordered phase of water on the MgO(100) surface: Low energy electron diffraction and helium atom scattering studies. *J. Chem. Phys.* **1996**, *105*, 1697−1701.
(15) Stirniman, M. J.; Huang, C.; Smith, R. S.; Joyce, S. A.; Kay, B. D. The adsorption and desorption of water on single crystal MgO(100): The role of surface defects. *J. Chem. Phys.* **1996**, *105*, 1295−1298.
(16) Giordano, L.; Goniakowski, J.; Suzanne, J. Partial dissociation of water molecules in the (3×2) water monolayer deposited on the MgO(100) surface. *Phys. Rev. Lett.* **1998**, *81*, 1271−1273.
(17) Włodarczyk, R.; Sierka, M.; Kwapień, K.; Sauer, J.; Carrasco, E.; Aumer, A.; Gomes, J. F.; Sterrer, M.; Freund, H.-J. Structures of the ordered water monolayer on MgO(001). *J. Phys. Chem. C* **2011**, *115*, 6764−6774.
(18) *Oxide Ultrathin Films: Science and Technology*; Pacchioni, G., Valeri, S., Eds.; Wiley-VCH: Weinheim, 2011.
(19) Pacchioni, G.; Freund, H. Electron transfer at oxide surfaces. The MgO paradigm: From defects to ultrathin films. *Chem. Rev.* **2013**, *113*, 4035−4072.
(20) Pacchioni, G.; Giordano, L.; Baistrocchi, M. Charging of metal atoms on ultrathin MgO/Mo(100) films. *Phys. Rev. Lett.* **2005**, *94*, 226104.
(21) Sterrer, M.; Risse, T.; Pozzoni, U. M.; Giordano, L.; Heyde, M.; Rust, H. P.; Pacchioni, G.; Freund, H.-J. Control of the charge state of metal atoms on thin MgO films. *Phys. Rev. Lett.* **2007**, *98*, 096107.
(22) Gonchar, A.; Risse, T.; Freund, H.-J.; Giordano, L.; Di Valentin, C.; Pacchioni, G. Activation of oxygen on MgO: O_2^- radical ion formation on thin, metal-supported MgO(001) films. *Angew. Chem., Int. Ed.* **2011**, *50*, 2635−2638.
(23) Starr, D. E.; Weis, C.; Yamamoto, S.; Nilsson, A.; Bluhm, H. NO_2 adsorption on Ag(100) supported MgO(100) thin films: Controlling the adsorption state with film thickness. *J. Phys. Chem. C* **2009**, *113*, 7355−7363.
(24) Hollerer, M.; Lüftner, D.; Hurdax, P.; Ules, T.; Soubatch, S.; Tautz, F. S.; Koller, G.; Puschnig, P.; Sterrer, M.; Ramsey, M. G. Charge transfer and orbital level alignment at inorganic/organic interfaces: The role of dielectric interlayers. *ACS Nano* **2017**, *11*, 6252−6260.
(25) Cabailh, G.; Lazzari, R.; Cruguel, H.; Jupille, J.; Savio, L.; Smerieri, M.; Orzelli, A.; Vattuone, L.; Rocca, M. Stoichiometry-dependent chemical activity of supported MgO(100) films. *J. Phys. Chem. A* **2011**, *115*, 7161−7168.
(26) Carrasco, E.; Brown, M. A.; Sterrer, M.; Freund, H.-J.; Kwapien, K.; Sierka, M.; Sauer, J. Thickness-dependent hydroxylation of MgO(001) thin films. *J. Phys. Chem. C* **2010**, *114*, 18207−18214.
(27) Newberg, J. T.; Starr, D. E.; Yamamoto, S.; Kaya, S.; Kendelewicz, T.; Mysak, E. R.; Porsgaard, S.; Salmeron, M. B.; Brown, G. E.; Nilsson, A.; et al. Autocatalytic surface hydroxylation of MgO(100) terrace sites observed under ambient conditions. *J. Phys. Chem. C* **2011**, *115*, 12864−12872.
(28) Shin, H.-J.; Jung, J.; Motobayashi, K.; Yanagisawa, S.; Morikawa, Y.; Kim, Y.; Kawai, M. State-selective dissociation of a single water molecule on an ultrathin MgO film. *Nat. Mater.* **2010**, *9*, 442−447.
(29) Wang, Z.-T.; Wang, Y.-G.; Mu, R.; Yoon, Y.; Dahal, A.; Schenter, G. K.; Glezakou, V.-A.; Rousseau, R.; Lyubinetsky, I.; Dohnálek, Z. Probing equilibrium of molecular and deprotonated water on TiO_2(110). *Proc. Natl. Acad. Sci. U.S.A.* **2017**, *114*, 1801−1805.
(30) Honkala, K.; Hellman, A.; Grönbeck, H. Water dissociation on MgO/Ag(100): Support induced stabilization or electron pairing? *J. Phys. Chem. C* **2010**, *114*, 7070−7075.
(31) Giordano, L.; Ferrari, A. M. Modified ion pair interaction for water dimers on supported MgO ultrathin films. *J. Phys. Chem. C* **2012**, *116*, 20349−20355.
(32) Pal, J.; Smerieri, M.; Celasco, E.; Savio, L.; Vattuone, L.; Rocca, M. Morphology of monolayer MgO films on Ag(100): Switching from corrugated islands to extended flat terraces. *Phys. Rev. Lett.* **2014**, *112*, 126102.
(33) Kresse, G.; Hafner, J. Ab initiomolecular dynamics for liquid metals. *Phys. Rev. B: Condens. Matter Mater. Phys.* **1993**, *47*, 558−561.
(34) Kresse, G.; Joubert, D. From ultrasoft pseudopotentials to the projector augmented-wave method. *Phys. Rev. B: Condens. Matter Mater. Phys.* **1999**, *59*, 1758−1775.
(35) Perdew, J. P.; Burke, K.; Ernzerhof, M. Generalized gradient approximation made simple. *Phys. Rev. Lett.* **1996**, *77*, 3865−3868.
(36) Grimme, S.; Antony, J.; Ehrlich, S.; Krieg, H. A consistent and accurate ab initio parametrization of density functional dispersion correction (DFT-D) for the 94 elements H-Pu. *J. Chem. Phys.* **2010**, *132*, 154104.
(37) Tersoff, J.; Hamann, D. R. Theory of the scanning tunneling microscope. *Phys. Rev. B: Condens. Matter Mater. Phys.* **1985**, *31*, 805−813.
(38) Hapala, P.; Kichin, G.; Wagner, C.; Tautz, F. S.; Temirov, R.; Jelínek, P. Mechanism of high-resolution STM/AFM imaging with functionalized tips. *Phys. Rev. B: Condens. Matter Mater. Phys.* **2014**, *90*, 085421.
(39) Savio, L.; Smerieri, M.; Orzelli, A.; Vattuone, L.; Rocca, M.; Finocchi, F.; Jupille, J. Common fingerprint of hydroxylated non-polar steps on MgO smoke and MgO films. *Surf. Sci.* **2010**, *604*, 252−257.
(40) Scamehorn, C. A.; Harrison, N. M.; McCarthy, M. I. Water chemistry on surface defect sites: Chemidissociation versus physisorption on MgO(001). *J. Chem. Phys.* **1994**, *101*, 1547−1554.
(41) Fernandes, E.; Donati, F.; Patthey, F.; Stavrić, S.; Šljivančanin, Z.; Brune, H. Adsorption sites of individual metal atoms on ultrathin MgO(100) films. *Phys. Rev. B* **2017**, *96*, 045419.
(42) Peng, J.; Guo, J.; Hapala, P.; Cao, D.; Ma, R.; Cheng, B.; Xu, L.; Ondráček, M.; Jelínek, P.; Wang, E.; et al. Weakly perturbative imaging of interfacial water with submolecular resolution by atomic force microscopy. *Nat. Commun.* **2018**, *9*, 122.

DOI: 10.1021/acs.jpcc.8b12256
J. Phys. Chem. C 2019, 123, 3711−3718